Chapter 3: HERA And H1

The HERA Accelerator

The Hadron Electron Ring Anlage (HERA) machine at Deutsches Elektronen-Synchrotron (DESY) in Hamburg is the first electron-proton (ep) colliding beam accelerator to be constructed. In previous experiments, electron-proton scattering has been performed using fixed targets. By going to a colliding beam arrangement, higher centre-of-mass energies can be achieved with the same beam energy. With HERA's design values of 30 GeV electrons on 820 GeV protons, the centre-of-mass energy is 314 GeV, equivalent to a 51 TeV electron beam in a fixed target experiment.

The rings that accelerate the two types of particle have approximately the same radius but have different designs. The electron ring uses normal magnets operating at room temperature whereas the proton ring uses superconducting magnets. This is because the designs of the two rings are driven by different limiting factors. For the electrons, the limiting factor is the rate at which they lose energy by synchrotron radiation as they traverse the curved sections of the ring. The rate of energy loss due to synchrotron radiation in a circular ring is given by

$$\Delta E = \frac{4\pi e^2}{3\rho}\,\beta^3\gamma^4$$

where ΔE is the energy lost per revolution, e is the charge of the particle, ρ is the radius of the ring in metres, β is given by $\beta=v/c$ where v is the particle's velocity and c is the speed of light in a vacuum and γ is given by $\gamma=(1-\beta^2)^{-1/2}$. For relativistic electrons, $\beta\approx1$ and only the γ dependence need be considered.

For a particle with momentum p,

$$\gamma = \frac{p}{mc\beta}$$

where m is the rest mass of the particle. Therefore, γ for an electron (rest mass 511 keV) will be about 2000 times larger than for a proton (rest mass 1 GeV) of the same momentum. As the

energy loss varies with γ^4, this effect is 13 orders of magnitude larger for electrons than for protons.

The limiting factor in building an electron ring accelerator is the ability of the radio-frequency cavities to pump energy into the beam to compensate for the energy loss in the curved sections. As there is an inverse dependence on the radius of curvature, it is advantageous to build a large ring to minimize this energy loss.

For the protons, the driving factor is how much bending field can be provided by the magnets. For a particle with charge 1, the radius of curvature ρ is related to the momentum of the particle p by

$$p = 0.3B\rho$$

where B is the field in Tesla, ρ is in metres and p is in GeV. For protons, which are not limited by energy loss, the maximum momentum achievable for a ring of fixed radius is therefore determined by the magnetic field that can be supplied by the magnets.

A summary of the HERA parameters is shown in figure 3.1. Both the design parameters and the parameters as achieved in the Autumn 1992 run are shown. Unfortunately, the 1992 run only produced 32 nb^{-1} of integrated luminosity compared with a design goal of 10^5 nb^{-1} per year. This has seriously limited the physics studies possible to date.

The accelerator chain for HERA is shown in figure 3.2. Protons are produced by stripping electrons from hydrogen ions produced by an H^- source. These ions are then accelerated up to 50 MeV in a linear accelerator (LINAC) and injected into DESY III, a new synchrotron. In this ring, protons are accelerated up to 7.5 GeV, then injected into PETRA. Here, they are accelerated up to 40 GeV before final injection into the HERA proton ring. Electrons (or in the future positrons) are accelerated to 400 MeV by another LINAC, then to 7 GeV in DESY II, then to 14 GeV in PETRA and finally injected into the electron ring of HERA.

The main purpose of HERA was to extend the range of deep inelastic scattering measurements to new regions of x and Q^2. Figure 3.3 shows the region which HERA will be able

to explore by running with 820 GeV protons on 30 GeV electrons (the electron energy for the 1992 run was 26.7 GeV rather than 30 GeV). There is no overlap between the region previously measured in fixed target experiments and the region measurable at HERA. This gap may be bridged by running with lower proton beam energies.

As shown in figure 3.2, the HERA ring itself is a flattened circle with a circumference of 6.3 km, consisting of four curved sections and four straight sections. The electron and proton beams may be brought into collision at four areas. Two of these areas contain large general purpose detectors: H1 in the North Hall and ZEUS in the South Hall.

Figure 3.1: Summary of HERA parameters. From [30].

Figure 3.2: The HERA accelerator chain.

Figure 3.3: The kinematic region accessible by HERA.

The H1 Detector

As outlined in the H1 technical proposal [31], a detector for HERA has to fulfil the following general requirements:

1) It must have a high degree of hermeticity in order to investigate phenomena involving energetic neutrinos or other non-interacting secondary particles.
2) It must permit good energy flow measurements for the inclusive measurement of neutral and charge current interactions. It must have good energy resolution, fine granularity and good absolute energy calibration for both electromagnetic and hadronic calorimetry.
3) Muon identification and measurement must be present for new particle searches, for heavy flavour studies and to preserve hermeticity when high-energy muons are present.
4) Electron identification and energy resolution must be good in order to use final-state electrons to reconstruct deep inelastic scattering event kinematics.
5) It must provide tagging of electrons which have emitted a photon in the detector and are therefore scattered through low angles in order to study photoproduction processes.

The H1 detector is described fully in [30]. The detector is shown in cut-away view in figure 3.4 and in longitudinal view in figure 3.5. The detector design is highly asymmetric as most of the final state particles are forced towards the incoming proton direction to conserve momentum. The centre of mass for HERA collisions is boosted with γ=2.86 along the proton direction with respect to the laboratory frame. This leads to a difference in the required instrumentation between the forward (incoming proton beam) and backward (incoming electron beam) directions.

In the following description of the H1 detector, the standard H1 co-ordinate system will be used. This is a right-handed Cartesian co-ordinate system with the origin at the centre of the detector, which is the nominal interaction point. The positive z direction is taken to be the proton direction. The positive x direction points to the centre of HERA and the positive y direction points upwards. This is shown in figure 3.6. The polar angle, θ, is then the angle relative to the beam axis and the azimuthal angle, ϕ, is measured from the x-axis.

Figure 3.4: The H1 detector, cut-away view.

Figure 3.5: The H1 detector, longitudinal view, showing the scintillator walls.

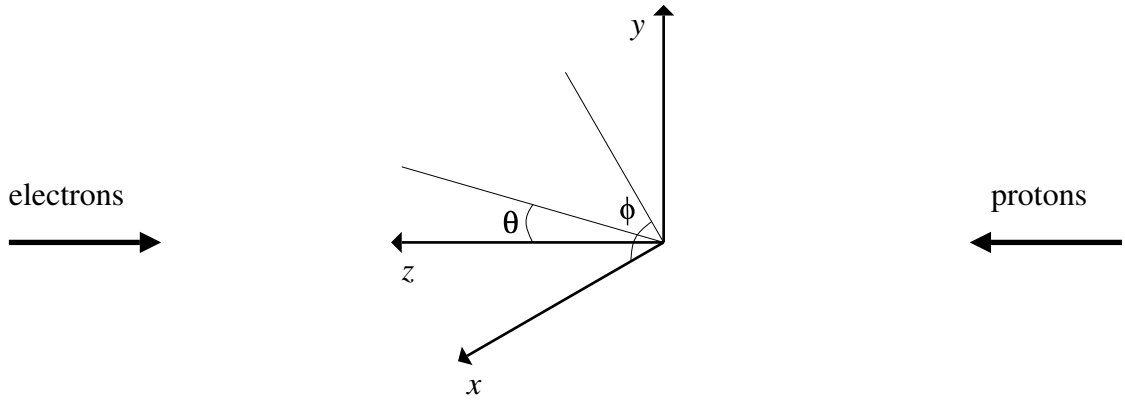

Figure 3.6: The H1 co-ordinate system.

The H1 detector consists of the following elements, proceeding outwards from the interaction point.

1) The beam pipe, having an inner diameter of 190 mm, with an aluminium wall 150 μm thick backed by 2 mm thick carbon-fibre reinforced plastic. A planned upgrade to H1 includes a vertex detector, for which a 45 mm inner diameter beam pipe will be used.

2) Tracking detectors, consisting of the central tracker (made of two jet chambers, two proportional chambers and two z chambers) and the forward tracker (made of three supermodules, each containing a radial chamber, a planar chamber, a multi-wire proportional chamber for triggering and a passive transition radiation layer).

3) Electro-magnetic calorimetry, consisting of a liquid argon-lead calorimeter in forward and barrel regions and the backwards electro-magnetic calorimeter, a lead-scintillator calorimeter, in the backwards region. A copper-silicon pad calorimeter (the Plug) closes the gap between the liquid argon calorimeter and the beam pipe in the forward region. The backwards proportional chamber is situated in front of the backwards electro-magnetic calorimeter and a scintillator wall for time-of-flight measurements is situated immediately behind.

4) Hadronic calorimetry, consisting of a liquid argon-stainless steel calorimeter in the forward and barrel regions.

5) The superconducting coil, which provides a 1.2T solenoidal field in the enclosed volume. For beam stability, a compensating magnet (with maximum field 6 T) is situated around the beam pipe to produce zero integrated field along the beam axis.

6) The warm iron return yoke for the solenoid, which is instrumented with limited streamer tubes to provide a tail-catcher for the hadronic calorimetry. The iron provides the only hadronic calorimetry in the backwards area as the liquid argon calorimeter extends only to θ=153°. The iron is also used as a muon filter and tracker, the field in the iron allowing a measurement of muon momentum to be made.

7) The forward muon spectrometer, consisting of drift chambers and an iron toroid, which is used to supplement the muon detection and momentum measurement in the forward direction.

8) Two scintillator walls (the large and small veto walls) situated at z=-6.5 m and z=-8.1 m from the H1 interaction point. These counters are used to aid in rejecting events caused by beam-wall or beam-gas interactions upstream of H1.

9) The electron and photon taggers, situated at z=-33.4 and z=-102.9 m respectively, which

are used to measure luminosity by measuring the rate of bremsstrahlung events. They are also used to tag photoproduction events with an electron in the electron tagger and no photon in the photon tagger.

The Central Tracking Detectors

The H1 tracking system is shown in figure 3.7. An end-on view of the central tracker is shown in figure 3.8. The central tracker is made from six individual detectors which were fabricated separately and then locked together to form the tracker unit.

Proceeding radially outwards from the beam, the first chamber is the Central Inner Proportional chamber (CIP). This is a multi-wire proportional chamber which provides space points for the Level 1 trigger and is read out using a pad segmented cathode with sixty pads in z and 8 in ϕ. The CIP has a double layer of chambers, formed by three concentric cylinders which are rotated by $\pi/16$ in ϕ with respect to each other. The wires run parallel to the beam with 480 wires in each layer. The chamber was operated with a 49.9% argon, 49.9% C_2H_6, 0.2% freon gas mixture in Autumn 1992. A time resolution of 21 ns was measured with test beams, and a similar performance was measured when the chamber was installed into H1. This resulted in a 2% chance of registering a given pad with the wrong (i.e. adjacent) beam crossing, giving a good signal for triggering.

The second chamber out from the beam is the Central Inner Z-chamber (CIZ). This drift chamber is designed to provide an accurate measurement of the z co-ordinate of tracks passing through the chamber as this co-ordinate is not well measured by the central jet chambers. The wires in the chamber are strung around the beam in sixteen sectors and the detector is subdivided into 15 rings in z. Each ring contains four sense wires and three potential wires. The precision of the z co-ordinate determination has been measured as 300 μm and the precision of the ϕ co-ordinate measurement performed by examining the pulses at both wire ends has been measured as 2.4% of the wire length (average wire length is 1120 mm). The maximum drift distance is 61.25 mm. The chamber was operated with an 80% argon, 20% methane gas mixture in 1992.

Figure 3.7: The H1 tracking system (*r*-*z* view).

Figure 3.8: The H1 central tracker, section perpendicular to the beam.

The third chamber is the inner Central Jet Chamber (CJC1). This chamber provides a good measurement of the position of tracks in the r-ϕ co-ordinates and a moderate measurement in z using charge division. The chamber is a jet chamber of the JADE type [32] with wires strung parallel to the beam axis but staggered at an angle of 30° with respect to the radial direction. Using this design optimises the track momentum resolution by ensuring that the ionisation electrons drift approximately perpendicular to the radial direction inside the H1 solenoidal field. It also allows resolution of drift ambiguities by connecting track segments of different cells. Each high-momentum track crosses the sense wire plane at least once in CJC1, allowing a determination of the passing time of the particle to 0.5 ns and giving a good trigger separation between beam crossings. Each plane of anode sense wires is surrounded by two adjacent cathode planes of wires shaping the drift field. An individual cell extends azimuthally from the sense wire plane to both cathode wire planes and radially over the whole of CJC1. CJC1 has 30 cells each with 24 sense wires. The resolution of CJC1 has been measured as 170 μm in r-ϕ and 2.2 cm in z. The chamber was operated with 89.5% argon, 9.5% CO_2 and 1.0% methane in 1992. The design of the chamber also allows a measurement of dE/dx, the specific energy loss, which is useful for particle identification. The resolution of the dE/dx measurement was measured as 10% for the Autumn 1992 run.

The fourth chamber is the Central Outer Z-chamber (COZ). This is similar to CIZ except that it is made up of 24 segments and 24 rings in z, with four sense wires and six potential wires per ring. The resolution in z has been measured as 200 μm and the resolution in ϕ was measured as 2% of the wire length (average wire length 2970mm). The maximum drift distance is 45 mm. The chambers were operated with a 50% argon, 50% C_2H_6 gas mixture in 1992.

The fifth chamber is the Central Outer Proportional chamber (COP) which is similar to CIP. The COP inner layer has 1574 wires and COP outer layer has 1615. COP has 16 pads in ϕ and 18 in z. The time resolution of COP was measured as 40 ns.

The sixth chamber is the outer Central Jet Chamber (CJC2). This is similar to CJC1 with 60 cells, each containing 32 sense wires. The chamber was run with the same gas mixture as CJC1 and was measured to have a similar resolution in r-ϕ, z and dE/dx.

The Forward Tracker

The forward tracker, shown in figures 3.7 and 3.9, is designed to measure tracks in the forward region, $5° < \theta < 30°$. It consists of three supermodules, each of which contains a planar chamber, a multi-wire proportional chamber (MWPC), a transition radiator and a radial chamber.

The planar chambers are constructed from three layers of drift chambers with parallel wires (perpendicular to the beam direction) each rotated by 60° from the previous layer in azimuthal angle. Each module contains 32 drift cells of identical rectangular cross section and wire lengths varying between 460mm and 1410mm. Each cell contains four sense wires, each surrounded by four grid wires on a 6 mm square matrix. The planars were operated with a gas mixture of 89% argon, 10% C_3H_8, 1% C_2H_5OH in Autumn 1992 and were measured to have a spatial resolution of 150 μm.

The radial chambers, which consist of wires strung radially, is split into 48 sectors in ϕ. Each sector is a drift cell having 12 sense wires, staggered alternately 287 μm either side of a plane which bisects the sector. Between adjacent sense wires, placed on the plane which bisects the sector, are field wires parallel to the sense wires. The sense wires of one sector are connected at the inner radius to the sense wires of the sector 105° away in ϕ. The reason for connecting two wires together is because it is not physically possible to site preamplifiers and electronics at the inner radius. A determination of the radial co-ordinate is still possible by using charge division, with a decision on which wire was stuck being based upon the charge division algorithm. The chambers were run with a 50% argon, 50% C_2H_6 mixture in 1992 although the design gas mixture is 40% helium, 40% C_2H_6, 20% xenon. The resolution achieved in 1992 was 180-200 μm in the drift co-ordinate and 3 cm in the charge division co-ordinate but it is expected that this will be improved in later runs.

In the 1992 run, the pattern recognition and reconstruction of tracks in the forward tracker was poor and therefore the forward tracker was not used in analysis of the early data. This situation has been remedied for the 1993 run.

Figure 3.9: The H1 forward tracker. a) Cross section in the *r*-*z* plane showing the three supermodules. b) Cross section in the *r*-ϕ plane showing the cell structure of each supermodule component in one quadrant.

The forward MWPCs are present to give fast signals for triggering purposes. They consist of two planes of wires interleaved with three cathode planes. The cathode pads are radially segmented into twenty rings and azimuthally segmented into sections covering $\pi/8$ except for the four outer rings which are segmented to cover $\pi/16$. Two consecutive cathode pads are offset by half a ring which effectively doubles the resolution in polar angle. The gas mixture used was 89.4% argon, 9.9% C_3H_8, 0.7% C_2H_5OH in 1992. For tracks crossing all three supermodules, the time resolution was measured to be 20 ns.

The last component of a supermodule is a transition radiator. This passive unit consists of an array of 400 polypropylene layers and is designed to aid electron-pion discrimination in the forward direction. Transition radiation occurs when a charge particle traverses an interface between media whose magnetic or dielectric properties differ [33]. If layers of radiating foils are arranged correctly, it is possible for interference to give rise to a threshold effect and for a given energy, electrons may be made to radiate while pions will not radiate.

The photons emitted by electrons traversing the foils are detected in the radial chambers, which are separated from the transition radiators by a thin window. The design goal is to achieve a 90% electron acceptance with less than 10% pion contamination for particles up to 80 GeV which pass through all three supermodules. Tests in a beam at CERN have shown that this is possible with the design 40% helium, 40% C_2H_6, 20% xenon gas mixture.

Liquid Argon Calorimeter

The liquid argon (LAr) calorimetry covers the forward ($4° < \theta < 20°$) and barrel ($20° < \theta < 152°$) regions. Both the electro-magnetic (EM) and hadronic liquid argon calorimeters consist of plates of metal (lead for the EM and steel for the hadronic) immersed in liquid argon. Both calorimeters are enclosed in a single liquid argon cryostat to avoid cracks and to minimise dead material.

Liquid argon calorimeters function by producing showers in the metal which then produce ionisation in the liquid argon gaps. The plates have electrodes attached to either side maintaining a potential difference in the gap. Thus, the electrons produced by the shower drift towards the positive plate and are amplified to produce an output signal proportional to the energy deposited in the gap. The plates are arranged in segments which are orientated to ensure that a particle coming from the interaction vertex is as near to normal incidence as practical (never more than 45° from normal incidence).

The segmentation of the calorimeter is shown in figures 3.10 and 3.11. The LAr is segmented along the beam axis into eight self-supporting wheels named IF, OF, FB2, FB1, CB3, CB2, CB1 and BBE for the EM calorimeter, which has no counterpart in the hadronic calorimeter. Each wheel is segmented into eight octants or stacks. The cracks between octants in the EM calorimeter point to the vertex in ϕ, but the cracks in hadronic calorimeters are designed not to point to the vertex in ϕ, as shown in figure 3.11.

Each electromagnetic stack consists of a pile of G10 (epoxy and fibreglass)-lead-G10 sandwiches separated by spacers to define the liquid argon gaps. The lead plates are 2.4 mm thick with 2.35 mm liquid argon gaps. Each gap has one readout plane and one high voltage plane. The total thickness of the EM calorimeter varies between 20 and 30 radiation lengths (X_0), as shown in figure 3.12.

Each hadronic stack consists of a pile of 19 mm stainless steel plates and 4.8 mm active gaps. In the middle of each active gap is a G10 board with pads on both sides. The high voltage planes are glued to the inner surfaces of the stainless steel plates. The hadronic calorimeter consists of between five and eight interaction lengths (λ) as shown in figure 3.12.

The energy resolution of the liquid argon calorimeter has been measured in electron and pion test beams and using data taken in place by H1. Figure 3.13 shows the energy resolution versus energy for electrons, figure 3.14 for pions. The parameterised form of the energy resolution, $\sigma(E)/E$, is

$$\frac{\sigma(E)}{E} = \sqrt{\frac{A^2}{E} + \frac{B^2}{E^2} + C^2}$$

where $A=11\%/\sqrt{E}$ $GeV^{0.5}$, B=154 MeV and C=0.6% for electrons and $A=(50.7\pm0.1)\%/\sqrt{E}$ $GeV^{0.5}$, B=0.9 GeV, $C=1.6\pm0.1\%$ for pions.

Figure 3.10: Longitudinal view of the H1 liquid argon calorimetry.

Figure3.11: A radial view of a single liquid argon calorimeter wheel.

Figure 3.12: Longitudinal view of the liquid argon calorimeter showing lines of iso-X_0 and iso-λ. The hatched areas in front of the calorimeters correspond to the material of the trackers and cryostat. All amounts of material are for a particle from the interaction point (IP). The dashed lines show the segmentation.

Figure 3.13: Energy resolution as a function of energy for electrons for wheels BBE, CB3, FB2 and IF. The solid line is the parameterisation of the energy resolution for FB2.

Figure3.14: Energy resolution as a function of energy for pions. The circles are for wheel IF only, the triangles are for wheel IF with the iron tailcatcher included. The solid line is a parameterisation of the resolution.

The Backwards Electro-magnetic Calorimeter And The Backwards Proportional Chamber

The Backwards Electro-magnetic calorimeter (BEMC), shown in figure 3.15, is designed primarily to measure electrons scattered at small angles in deep inelastic scattering. The BEMC covers the angular range $151° < \theta < 177°$. The BEMC is a lead-scintillator calorimeter in which the showers produced in lead plates cause ionisation of atoms in the scintillating material, resulting in the production of light as the ions and electrons recombine.

The BEMC contains 88 calorimeter stacks aligned parallel to the beam line. There are 56 stacks with a square cross-section, the others being trapezoidal or triangular in order to fill the circular barrel. The basic layer consists of 2.5 mm of lead followed by 4 mm of plastic scintillator. Each stack contains 50 layers, corresponding to 22.5 radiation lengths.

The BEMC is read out via a 0.3 mm air gap to wavelength shifter bars. Two pairs of 8 cm bars cover two opposite sides of a square stack and extend over the full active length. The remaining two sides are covered by 16 cm wide bars which cover only the last 15 sampling layers in the stack, giving access to the tails of showers (the last 6.8 radiation lengths). The light emitted in the wavelength shifters is then read out by photo-diodes (one per bar).

The BEMC resolution has been determined in test beams to be $10\%/\sqrt{E} \oplus 1\%$. The average noise per calorimeter stack has been measured as 150 MeV. The uncertainty in calibration between stacks has been estimated as 3%. The position resolution for electrons has been measured to be 1.3 cm.

As the H1 hadronic liquid argon calorimeter does not cover the backward area, the BEMC must be used in conjunction with the iron tailcatcher to provide a measurement of hadronic energy flow. However, as the BEMC only corresponds to 0.97 hadronic interaction lengths, using the BEMC for hadronic calorimetry is problematic. About 30% of all hadrons do not produce any showers in the BEMC and their minimum-ionising signal is not detectable above the noise. When a hadron does produce a shower in the BEMC, only about 30% of the energy of the shower is contained within the BEMC. A hadronic energy resolution of $80\%/\sqrt{E}$

has been determined from simulation but a full study of the real detector's hadronic response is still in progress.

The Backwards Proportional Chamber (BPC) consists of five graphite cathode planes on Mylar foil and four anode wire planes. The BPC sits on the front face of the BEMC to improve the position resolution for scattered electrons and to provide trigger signals. Unlike the other H1 MWPCs, the BPC cathode is not segmented and the anode wires are read out. The wires are strung every 2.5 mm, perpendicular to the beam, and are horizontal, vertical, +45° and -45° for the four planes. The chamber was operated with a gas mixture of 49.9% argon, 49.9% C_2H_6, 0.2% in 1992. The points given by the BPC lead to an angular resolution of 0.5 mr, the same order of magnitude as the deviation of a particle's trajectory caused by multiple scattering in the material between the interaction point and the BPC. The time resolution of the BPC has been measured as 20 ns.

Figure3.15: The Backwards Electromagnetic Calorimeter, BEMC (*x*-*y* view).

The Plug Calorimeter

The plug calorimeter is designed to fill the gap in acceptance between the liquid argon calorimeter, which ends at $\theta=3°$, and the beam pipe, which begins at $\theta=0.6°$. The plug is a silicon-copper detector, where the silicon is used as a reverse-bias diode with a large depletion region. Showers produced in the copper produce electron-hole pairs in the silicon which are collected to give the signal. The energy resolution for hadrons has been measured as $150\%/\sqrt{E}$. The plug was not fully instrumented for the Autumn 1992 run and it will not be discussed further.

The Instrumented Iron

The instrumented iron serves three purposes in H1. Firstly, it acts as a return yoke for the superconducting solenoid. Secondly, it acts as a tail-catcher calorimeter to contain hadronic showers that escape from the liquid argon calorimetry. Finally, the iron acts as a muon filter and allows a measurement of muon momentum to be made as the iron is magnetised.

In order to be able to measure hadronic energy flow, the iron has gaps in it containing gas counters operated in limited streamer tube mode. These tubes are oriented along the beam axis in the barrel region ($25° < \theta < 130°$) and vertically in the forwards and backwards endcaps. The tail catcher covers the angular region $5° < \theta < 175°$. Of the 16 layers of streamer tubes in the iron, 11 are equipped with readout pads varying in size from 30 cm x 30 cm in the endcaps to 50 cm x 40 cm in the barrel region. The pad signals from the five inner and six outer layers are summed to form inner and outer towers. The energy resolution for hadrons has been measured as $100\%/\sqrt{E}$.

Muon measurement is provided by muon boxes. Inside the inner radius of the iron is a muon-box consisting of three layers, two strip layers with strips perpendicular to the wire direction and one pad layer. Pad layers are also installed in the first three iron slits for the calorimeter. The fourth slit is twice the width of the others and contains two chamber layers, one pad and one strip. Pad layers are inserted in the remaining five slits and another muon-box is attached to the outside of the iron.

The instrumented iron chambers were operated with a 88% CO_2, 2.5% argon, 9.5% isobutane gas mixture in 1992. The detector resolution for space points was measured to be 10 cm for the pad readout tubes, 3-4 mm for wire hits and 10-15 mm for strip hits.

The Forward Muon Spectrometer

The Forward Muon Spectrometer is designed to provide muon tagging and momentum measurement in the forward region, $3° < \theta < 17°$, and will be discussed in detail in chapters four and five.

The Time-Of-Flight Device And The Veto Walls

The time-of-flight (TOF) device, shown in figure 3.16, consists of two scintillator walls situated behind the BEMC. The function of the TOF is to provide timing information for the level one trigger in order to be able to reject proton beam related backgrounds. Losses from the beam occur due to the protons interacting with residual gas in the beam pipe and interactions between off-momentum beam particles and the wall, producing showers of hadrons and halo muons which can extend for 30 m or more along the beam direction. It is expected that H1 will typically be hit by such background events at a frequency of 2.6 MHz.

Each of the two TOF walls consists of a 3 cm thick layer of plastic scintillator sandwiched between two 6.5 mm thick lead layers, mounted on a backing plate of non-magnetic steel. The lead, corresponding to 1.1 radiation lengths, absorbs synchrotron radiation, protecting the counters and limiting the background rates. The TOF is read out by photo-multiplier tubes.

The TOF has been measured to have a time resolution of 4 ns, although the individual counters were found to have a resolution of 2 ns. The TOF provides a trigger signal within 250 ns of an interaction occurring. Figure 3.17 shows a typical time distribution of hits in the TOF and clearly illustrates the discrimination that is possible between background events and data events.

The large and small veto walls are situated at z=-6.5 m and z=-8.1 m respectively, as

shown in figure 3.5. These counters consist of double layers of plastic scintillator and are designed to provide additional time-of-flight information for background rejection. The small (or inner) veto wall covers the region near the beam pipe down to a radius of 11 cm. The large (or outer) veto wall overlaps the inner veto wall and most of the instrumented iron endcap. There is a 3m thick concrete wall between the large veto wall and the H1 detector.

Figure 3.16: The TOF device.

Figure 3.17: Time distribution of hits in a TOF counter, showing a clear discrimination between background and data.

The Luminosity System

The H1 luminosity monitor consists of two counters, an electron (e) tagger located at $z=-33.4$ m and a photon (γ) tagger at $z=-103$ m. The counters are placed close to the beamline in order to detect particles scattering through small angles at the interaction point. The luminosity is determined by measuring the rate of Bethe-Heitler events (i.e. $ep \rightarrow ep\gamma$), which have an electron in the electron tagger and a photon in the photon tagger.

The luminosity system is shown in figure 3.18. Scattered electrons are deflected by a set of quadrupoles and a bending magnet such that they pass through an exit window at $z=-27.3$ m to hit the electron tagger. The bremsstrahlung photons leave the proton beam pipe through the photon exit window at $z=-102.9$ m, pass through a two radiation length lead filter followed by a one radiation length water Cerenkov counter before hitting the photon detector. The lead protects the counter from the high flux of synchrotron radiation. The Cerenkov counter is used to detect whether the photon has passed through the lead without interacting.

The luminosity detectors are total absorption Cerenkov calorimeters made of KRS-15 crystals (78% TlCl and 22% TlBr). They correspond to 0.93 radiation lengths and have a crystal length of 20 cm. The energy resolution of both counters has been measured as $10\%/\sqrt{E}\oplus 1\%$ and the time resolution as 3 ns. The position resolution has been measured as 0.3 mm for the electron tagger and 1.2 mm for the photon tagger.

In addition to their luminosity measuring function, the counters may be used to trigger on photoproduction events where the scattered electron is detected in the electron tagger. The acceptance of the luminosity system, summarised in figure 3.19, allows the detection of such events with $Q^2<0.01$ GeV^2 and $0.2 < y < 0.8$.

Figure 3.18: The H1 luminosity monitoring system.

Figure 3.19: The acceptance of the luminosity system.

Trigger and Data Aquisition

The H1 trigger system was designed to distinguish electron-proton collisions from background processes at a rate which is comparable with the time taken for the next bunch crossing to occur. Typical background processes are caused by off-momentum protons hitting the beam wall and other components, protons interacting with residual gas nucleii and synchrotron radiation from the electron beam. As the rate of ep collisions is small compared with the background rate, the trigger has to be very efficient at keeping ep events but at the same time remove a large fraction of the background events.

The ep collisions should occur within the fiducial volume of the ep interaction region (i.e. within ≈1m of the nominal interaction point). In contrast, beam-wall and beam-gas interactions may take place anywhere and hence those outside the fiducial volume may be rejected. The remaining backgrounds within the fiducial region may be rejected by making further requirements on the event topology. Hard scattering events have a higher total transverse energy than background events. Charged-current deep inelastic scattering events may be identified by searching for missing transverse energy and neutral-current deep inelastic scattering events may be identified by searching for isolated energy deposition in the calorimeters from the scattered electron. Photoproduction events may be triggered by requiring an electron in the e-tagger and no photon in the γ-tagger. Heavy flavour states producing muons may be triggered by searching for muon candidates in the instrumented iron and forward muon spectrometer.

All detector readout is first performed into 'pipelines' which store the digitised signals until a trigger 'keep' signal (i.e. a signal to accept the event) is received or until the pipeline can no longer store the information. This system was necessary to allow H1 to trigger at a beam crossing interval of 96 ns without introducing deadtime in the level one trigger.

The level one trigger consists of nine different trigger systems, each based on the information from a single sub-detector. The output of these systems are called trigger elements, which are then combined in the central trigger logic to supply various subtriggers. Each subtrigger produces a level one keep signal which stops the pipelines and prepares the event to

be read out. The most important level one trigger elements are:

1) The TOF trigger, which uses the TOF counter signals to produce a powerful discrimination between 'in-time' interactions in the fiducial volume and 'out-of-time' interactions elsewhere. The TOF background trigger element is the most effective background rejection criterion and is therefore applied as a veto to many physics sub-triggers.
2) The *z*-vertex trigger, which uses the CIP, COP and the first forward MWPC to find sets of hits (called rays) consistent with the passage of a particle through the detector. The *z* origins of the rays are then examined to determine the position of the event vertex. Another important trigger element is *z*-vertex*t0, which indicates that there is at least one ray in the tracking (i.e. that there is some activity in the centre of the detector).
3) The forward ray trigger, which finds rays in the forward MWPCs and CIP.
4) The MWPC triggers, which includes the CIP trigger (used to provide triggers for taking cosmic muon data) and the BPC trigger (which looks for coincident hits in at least three out of four BPC layers). The CIP trigger may also be used to search for rays pointing mainly backwards which may indicate a proton-gas interaction upstream.
5) The big ray trigger, which looks for combinations of rays from *z*-vertex and forward ray triggers.
6) The CJC triggers, used principally to find rays in the CJC that have a distance of closest approach to the beam axis of less than 2 cm. Tracks with high and low transverse momentum can be distinguished. Topological requirements may be made on the rays, such as requiring two rays to be back-to-back in ϕ.
7) The *z*-chamber trigger, which uses CIZ and COZ to find rays and hence measure the position of the interaction vertex.
8) The liquid argon calorimeter trigger, which provides triggers based on transverse and total energy as well as allowing various topological signals to be identified using lookup tables.
9) BEMC Single Electron Trigger (BSET) which looks for an isolated electron in the BEMC.
10) The Instrumented Iron trigger, which looks for muons in the iron.
11) The forward muon trigger, which looks for muons in the forward muon spectrometer. The

operation of the trigger system for the forward muon system will be described in greater detail in chapter four.

12) Luminosity triggers, principally ETAG, which searches for an electron in the electron tagger and no photon in the photon tagger.

The level two trigger is used to decide quickly (within 20 μs) whether the event should be kept or rejected. Once a level two trigger keep signal has been produced, readout of the detector proceeds, extracting the data stored in the pipelines. The level two trigger includes topological and neural net triggers, but was not available for the Autumn 1992 run and so will not be discussed further. Similarly, the level three trigger, which runs on AM 29000 RISC processors, is able to assemble more information for a better trigger evaluation. This was also not installed for the Autumn 1992 run.

The level four trigger is a filter farm based on fast mips R3000 processor boards. It is integrated into the central data acquisition system and performs a cut-down version of the full event reconstruction online to allow a powerful discrimination on the basis of physics class. In the Autumn 1992 run, the filter farm was mainly used to reconstruct the event vertex from the CJC information and reject those events with a vertex outside the fiducial volume.

The H1 data acquisition system is shown schematically in figure 3.20. It is based mainly on the IEEE VMEbus standard [34]. Information is read out in parallel from each subdetector system before being combined into a single event record by the event builder. Data compression is carried out online to reduce the volume of data from 3 MBytes of raw data down to event sizes of between 50 KBytes and 100 KBytes. Fast data transmission is provided by a VMEtaxi optical bus. Control of the experiment is provided by several Macintosh computers in the H1 control room. These computers do not actually perform any of the data aquisition tasks, which are handled by processors in crates, but they do provide control of parameters and monitoring of the experiment.

Figure3.20: The H1 data acquisition system.

The Data Processing System And Reconstruction Software

The data taken by H1 are stored on raw data tapes on the DESY IBM 9000/720 VF mainframe. This machine is used, together with a robot tape silo, to store, manage and export all of the experiment data (raw, reconstructed and simulated). The reconstruction program for H1, H1REC [35], runs offline on many platforms but the production reconstruction is done by a semi-online system consisting of three Silicon Graphics 4D/460 workstations with six processors each. This processing produces Production Output (POT) tapes from the raw data. A cut-down version of H1REC also runs on the level four trigger filter farm. Data analysis is carried out on the DESY IBM, on Hewlett-Packard workstations and on the Silicon Graphics machines. Data Summary Tapes (DSTs) consisting of event selected on the basis of physics class are exported to outside institutions for further analysis work.

H1 software is principally written in FORTRAN 77, with the exception of the QT analysis program H1QT [36] which is written in C as the code has to run on front-end processors as well as offline machines. The code is managed using the CMZ code manager [37]. Memory management is provided by the BOS package [38] with additional discipline provided by a data definition language [39]. All data are contained in BOS banks, which are tabular arrays of values and pointers to related rows in other tables. Steering through the relations of a bank is performed by DATMAN, a tool written for this purpose [40]. Machine-independent input-output is provided by the FPACK package [41].

All H1 software has been written in a modular fashion. A module is a self-contained set of routines that perform their own initialisation upon first call and thereafter operate on input BOS banks to produce output BOS banks. A module is not allowed to change its input banks, nor is a module allowed to change the output banks produced by a different module. A large program such as H1REC therefore consists solely of a number of module calls to each of the subdetector reconstruction systems. The operation of a module may be controlled by steering banks, a BOS bank with just one row that supplies parameters to the code when run. These banks are stored as text files and are read in at the start of a job, so that reconstruction parameters may be changed without re-compiling the code.

The calibration constants, geometry and run summary information are all stored in BOS banks. A purpose-written database MDB [42] holds all this information and provides mechanisms for marking the range of validity for different versions of a bank. The database also contains default version of steering banks. The database also allows update and inspection of the calibration constants.

The Simulation Software

The H1 simulation program H1SIM [43] is based on the GEANT package [44]. The geometry of the detector and beamline within 100 m of the interaction point has been implemented with two levels of granularity to allow faster simulation when maximum accuracy is not required. The granularity of each detector component is controlled by a steering bank, as is the information produced by each sub-detector volume. In addition, components may be switched off to allow detailed simulation of single detector components.

In order to provide accurate detector response simulation, especially with fine geometry, it is necessary to keep track of particles with kinetic energies as low as 1 MeV. This leads to a simulation time of 600 s for a typical deep inelastic scattering event on a Silicon Graphics 4D/460 processor. To help contain the CPU requirement, the tracking step (where all particles are tracked through the subdetector volumes and energy deposition recorded) is separated from the digitisation step which simulates the detector response to this energy. This allows limited re-processing for different calibration constant without repeating the tracking step. The trigger simulation step is also separated so it can be repeated without duplicating the digitisation step.

A fast parameterisation of energy showers in the calorimeters, H1FAST [45], was developed and implemented. This suffices for non-critical applications as the detailed shower profiles are not generated, saving a factor of 10 in CPU time. Finally, for relatively coarse work such as feasibility studies, an ultra-fast parameterised simulation program called H1PSI [46] was developed. This program has a simulation time of about 0.1 s on a Silicon Graphics 4D/460 processor.

The Physics Analysis Software

H1 has two physics analysis tools. The first of these is LOOK [38], a graphics package which provides histogramming functions and also provides a user-friendly, machine independent interface with the low-level graphics primitives used (currently GKS [47]). The LOOK system runs on many platforms, including the Macintosh computers that monitor data acquisition in the H1 control room. The H1 event display H1ED [48] is written within the LOOK framework and allows histogram analysis to be performed whilst scanning events. H1ED can also call any H1 modules, for example, to repeat the digitisation step of the current simulated event with a new set of calibration constants.

The second package for physics analysis is called H1PHAN [49]. This program is essentially a subroutine library that operates on four-vectors which are constructed by the H1PHAN program from the reconstruction output banks. H1PHAN includes a large number of standard routines such as Lorentz transformations, deep inelastic scattering kinematics and jet finding algorithms, allowing these to be maintained centrally and avoiding duplication of effort. The user of H1PHAN writes his own subroutines for physics analysis work which can call any of the standard routines. H1PHAN is usually used to produce histograms for interactive analysis in LOOK.